Heliyon 10 (2024) e26666

Contents lists available at ScienceDirect

Heliyon

journal homepage: www.cell.com/heliyon

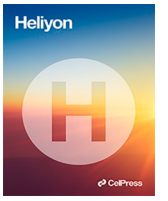

Research article

Identification of 2-d shape parameters for waste brick powders from varying milling methods: A discussion of quantitative image analysis

David Sinkhonde

Department of Civil and Construction Engineering, Pan African University Institute for Basic Sciences, Technology and Innovation, Nairobi, Kenya

ARTICLE INFO

Keywords:
Shape parameters
Scanning electron microscopy
Waste brick powder
Morphology
Quantitative image analysis
Pozzolanic materials

ABSTRACT

Quantitative characterisation of morphology and shape parameters of pozzolanic materials, as a fundamental problem of characterisation of pozzolanic materials, has received significant consideration in literature. Thus far, previous research works have not paid much attention to the circularity, roundness and solidity of pozzolanic materials including waste brick powder (WBP). This research makes a significant contribution on identification of circularity, roundness and solidity of WBP particles under milling conditions using quantitative image analysis. In particular, the goal was to interrogate the ball milling treatment variables for generating WBP using scanning electron microscopy (SEM) and image analysis. Under the milling conditions of changing sample masses introduced in ball mill, the average circularity values for the specimens were approximately 0.6 whilst the average solidity values for the specimens were approximately 0.71. Moreover, the average roundness values for the specimens were nearly 0.51. It was shown that the trends of shape parameters of WBP under changing fineness levels were not significant. The values of circularity, solidity and roundness in this study therefore collaborate to support the discoveries of hidden shape characteristics of WBP specimens and can tackle the overall behaviour of cement-based composites containing WBP. Quantitative image analysis was therefore observed to be capable of inheriting detailed information from SEM micrographs and remains one of the most outstanding approaches of generating shape parameters.

1. Introduction

In these recent years, the particle shapes of pozzolanic materials have attracted the increasing interest of researchers due to their influence on the behaviour of cementitious composites [1]. The field of cementitious composites, which considers the reaction between pozzolanic materials and cement, is undergoing active developments. This field aims at understanding the roundness of particles which is accompanied with the smoothness of corners or angles of the particles [2]. The particle shape characterisation activities of pozzolanic materials have focused on the spherical particles of fly ash, which in turn affect the workability of concrete and grout and have significant influence on hot mix asphalt applications [3]. The characterisation activities of particle shapes also focus on applications such as influence of particle shape and fineness of metakaolin on water demand of cementitious composites [4–7], dependency of workability properties on incorporation of silica fume in cement-based composites [8–10], correlation between surface areas of rice husk ash (RHA) and ground granulated blastfurnace slag (GGBS) and their particle shapes [11] and changes of particle shapes of GGBS

E-mail address: sinkhonde.david@students.jkuat.ac.ke.

https://doi.org/10.1016/j.heliyon.2024.e26666
Received 29 August 2023; Received in revised form 14 February 2024; Accepted 16 February 2024
Available online 17 February 2024

using varying grinding conditions [4]. At the moment, this area of study is very extensive and the afore-stated references and examples might not give an exhaustive overview. While grinding essentially dictates the shape particles of pozzolans such as GGBS, the relationship between grinding of clay bricks using different masses and particle shapes of the generated WBP remains relatively unexplored.

The quantitative characterisation of shape parameters of pozzolanic materials is a key step in fundamental challenges for characterisation of solid powders. This has been a topic of substantial attention in several problems of material characterisations in literature [2,12–17], to cite a few. Most of these studies deal with general properties of powders generated after grinding. Only few studies are available on characterisation of particle shapes of pozzolanic materials using various grinding conditions. Examples include the analysis of grinding on particle morphological shapes of fly ash and GGBS [4,18]. It is known that the morphological properties of particles are established based on various scales including surface texture (small scale) and shape (medium scale) [2]. Although scanning electron microscopy (SEM) is increasingly becoming a prominent method for identifying the morphology of materials including pozzolans [19–26], the predicted data of surface texture and shape using SEM can be inaccurate and its use has been faced with drawbacks [26]. Quantitative estimation of shape and surface texture using SEM is even more problematic when material characteristics are complex [26]. In several real applications, the material properties are usually complex, thereby requiring other methods that can couple with SEM. Alternatively, quantitative electron count method in SEM has opened the way for evaluating quantitative information of morphology of particles but magnification and small sized particles would oblige to conduct additional techniques for generating morphology of particles [26]. Fortunately, SEM images can be exploited further for easing the identification of shape parameters (e.g. roundness, circularity, solidity etc.) [1]. In this paper, the analysis of milling conditions of clay bricks is addressed around the shape parameters of roundness, circularity and solidity of waste brick powder (WBP).

Huge efforts have been undertaken by researchers in order to determine the shape parameters of particles. This has opened doors to several methods which are available for analysis and quantification of shape parameters. Some of these methods include the use of commercial image processing software programmes (e.g. Aphelion and Image-Pro Plus®) and use of advanced programming languages or software (e.g. Visual Basic, C++ and Matlab) [27–29]. By these approaches, the basic characteristics of particle shapes are successfully analysed. Note that the free and open source image analysis has for example increasingly been considered as a formidable contender to the aforesaid methods, where ImageJ was used for identification of food grains elsewhere [30]. Literature shows that ImageJ is commonly implemented software in image processing and it uses vital components such as histogram manipulations (see Refs. [1,15,29–37] and the references therein). In some cases, it calculates the extents of dispersions of nanomaterial particle sizes and silicate layers [33,38]. Representative examples of independent shape parameters are solidity, axial ratio, sphericity, roundness and circularity. Research on particle shapes of materials is aimed at classifying the particles by differentiating the morphological types and constituents [39]. Circularity is a parameter that is generated from 2-d microscopic views and has been regularly computed instead of sphericity as its measurement is easier [40]. The outcome of circularity of 1 indicates a perfect circle while a circularity of approximately 0 shows increasingly elongated shapes. On the other side, solidity values quantified as the ratios of particle areas to the values of convex hull, investigate the whole particle concavity [41]. A solidity value of nearly 1 indicates a particle with smooth outlines whilst a solidity value that is approximately 0 shows a particle with rough outlines.

In earthen construction and concrete production, the use of pozzolanic materials is attractive due to their low costs and pozzolanic properties which control the partial replacements of cement [42–44]. The predominant advantages of the use of pozzolanic materials in cement-based composites emerge from the readily availability of the materials in many countries. The other important driving factor for use of pozzolans in cement-based composites is the massive production of cement which is accompanied by challenges of environmental pollution [45]. While material compositions of pozzolans dictate the overall behaviour of cement-based composites [46,47], their morphology and shapes also contribute to the performance of pozzolans in cementitious composites [11]. This explains why examinations of mineral compositions, morphology and shapes of pozzolans have been at the forefront of various research works [11,48–55]. In these cited studies, the different properties of pozzolans were used to engineer the different mechanical properties of cement-based composites. Regardless of methods used in characterising pozzolans in literature, the underlying goal of such characterisation is to promote the performance of cement-based composites containing pozzolans. This research fills some gaps in literature by showing that particle shapes of WBP under grinding conditions can be identified with SEM, but this does not offer significant quantitative data on circularity, roundness and solidity. In this case, the solution could be to employ quantitative image analysis and illustrate such particle shapes explicitly. Likewise, the study demonstrates that extending the charaterisation of WBP particle shapes such as circularity, roundness and solidity is a significant advancement since properties of cement-based containing pozzolanic materials also rely on such particle shapes [4,18,56].

It is known that the particle sizes and morphology of pozzolanic materials have been well studied, as discussed previously. However, much less is known on the particle shapes of circularity, solidity and roundness for WBP particles under conditions of grinding. Building upon the earlier research works, the goal of this research is to learn about the approach of quantifying shape parameters of WBP generated using varying milling conditions. The studies of shape parameters of pozzolans in literature [4,7–9,11], have brought about considerable information on characterisation of pozzolanic materials. In some cases, the shape parameters of pozzolanic materials have turned out to be very significant in cementitious composites, thus influencing the behaviour of cementitious composites [4,18]. Yet up to now the study of circularity, roundness and solidity of WBP particles under milling conditions does not exist. This paper intends to make one step in this direction by first presenting how the circularity, roundness and solidity properties of WBP change under milling conditions. As another important practical outcome, this study emphasises heavily on results from combination of SEM and quantitative image analysis. It becomes very clear that the presentation of this approach, like other shape identification methods, should be economical without violating the validity of the results.

2. Materials and methods

2.1. Materials

The specimens used in this research were ordinary Portland cement (OPC) CEM I with specific gravity of 3.12 and WBP with a specific gravity of 2.69. Fragmented clay bricks used for generating WBP were collected from Kenya Clay Products factory. Clay bricks at this factory were burnt at 950 °C. OPC used in this study was class 42.5 in conformity with the British standard specification [57]. Generating WBP encompassed grinding of clay bricks with a ball mill using changing masses of clay bricks (8, 9, 10, 11 and 12 kg). The grinding speed and grinding time were maintained as 1260 rpm and 1 h, respectively. The ground WBPs were sieved and the specimens that passed through 0.075 mm sieve were used for scanning electron microscopy experiments.

2.2. Methods

2.2.1. Chemical compositions

X-ray fluorescence (XRF) test is implemented to evaluate the elemental compositions of materials. Information of elemental compositions is generated using an XRF gun and it is frequently employed because of its excellent characterisation approaches apart from its economic benefits [58]. The fundamental ingredients of XRF tests are voltage and current ranges of 30–60 kV and 0–100 mA, respectively. In this work, a bruker spectrometer gun was employed for quantifying the elements available in WBP. For the sake of comparisons, the chemical compositions of OPC were also determined. Moreover, the loss on ignition (LOI) values were determined after burning the specimens at 800 °C for 45 min in conformity with the code [59].

2.2.2. Scanning electron microscopy

SEM was introduced to address the morphology and shape parameters of OPC and WBP. The process of scanning the specimens employed JEOL NeoScope JCM-7000 SEM equipment (Fig. 1). SEM allows the assessment of powders and solid objects and has been considered as the most extensively utilised method in material characterisation [60,61]. To reach this goal, SEM uses electron beams to obtain morphological details of the surface. For this application, the samples were dried and cleaned before SEM assessment to increase the exposure of the surfaces. After this preliminary step, the specimens were sprinkled on the conductive adhesive tape and positioned appropriately in the sample chamber. Afterwards, the micrographs were generated using electron beam which scanned the surfaces of the specimens.

2.2.3. Quantitative image analysis

The functions of solidity, roundness and circularity were built from the knowledge of SEM micrographs and these were evaluated using ImageJ. Since it is challenging to obtain quantitative information of shape parameters of specimens using SEM alone, quantitative image analysis ensured the fulfilment of such details. To run ImageJ, Java runtime environment (JRE) and additional functional programmes such as macros and plugins are needed [32]. Comprehensive procedures required during generation of shape parameters are presented elsewhere [32,62,63]. The shape descriptors including their mathematical expressions and sensitivity are exhibited in Table 1. The abbreviations summarising the shape descriptors are presented in Table 2. Throughout the manuscript, the shape parameters are constantly referred to circularity, solidity and roundness. The values of circularity, solidity and roundness evaluated in this research were less than 1.

Fig. 1. A scanning electron microscope.

Table 1
Shape descriptors, sensitivity and mathematical expressions.

Shape descriptor	Mathematical expression	Sensitivity	Reference
Circularity	$\frac{Pp}{2\sqrt{\pi Ap}}$	Form and roughness	[64,65]
Roundness	$\frac{4Ap}{\pi Dmaxferet^2}$	Form	[66]
Solidity	$\frac{Ap}{Ach}$	Roughness (morphological)	[67]

Table 2
Summary of abbreviations.

Symbol	Definition
Pp	Particle perimeter
Ap	Particle area
Ach	Convex hull area
$D_{maxferet}$	Maximum Feret diameter

3. Results and discussion

3.1. Chemical compositions

The results obtained with the approach of chemical composition tests for OPC and WBP are shown in Table 3. This section explores if the pozzolanic properties of WBP complied with specifications in the standard [68]. In this case, the required pozzolanic properties specified in the code [68], are reachable. This is justified by the fact that the sum of compositions of SiO_2, Fe_2O_3 and Al_2O_3 is greater than 70% as required in the code [68]. On the other hand, the lack of MgO in OPC in this work proves excellent soundness characteristics [69]. It is shown that, with the content of magnesium oxide being less than 5% as specified in the standard [57], no failure of OPC in soundness can be provoked.

As shown in Table 3, all the oxides estimated in OPC are also noticed in WBP and are in conformity with the observations of other researchers [70]. As clearly shown in Table 3, the outcomes of ($SiO_2 + Fe_2O_3 + Al_2O_3$) of greater than 70% indicated in the standard [68], are confirmed here thanks to burning the clay bricks at 950 °C. The consideration of LOI of WBP can also be traced from Table 3 which indicates the value less than 10% as a limit in the standard [68]. The findings in Table 3 therefore confirm that WBP attains the pozzolanic state and can participate in pozzolanic reaction once blended with OPC. Since this work concentrates on shape parameters, comprehensive discussion on pozzolanic reactivity of WBP is left out in the rest of the paper. The interested reader is referred to detailed discussion in literature [71,72].

3.2. Scanning electron microscopy

Fig. 2(a–f) reports the micrographs of OPC and WBP specimens generated using SEM. The reason for introducing SEM was to explore the particle surface texture and particle shapes from the visual assessment point of view. The method is particularly important in exploring the size, morphology and formation of specimens after probing them on fine scaling [73,74].

As depicted in Fig. 2(a–f), the surface textures and particle shapes of the specimens are noticed. In this work, detailed discussion about surface texture is left out for the sake of brevity. Such discussion can be found in literature [51,72,75]. Only detailed discussion of particle shapes of the specimens is presented. It is important to highlight that it is difficult to estimate the shape parameters of WBP using SEM only in Fig. 2(a–f). In order to enhance the quantitative information of the specimens, quantitative image analysis was employed and discussions on findings from such method are presented in the subsequent sections. Quantitative image analysis will investigate the significance of changing masses of clay bricks introduced in ball mill, both in terms of advantages and disadvantages of such method.

Table 3
The chemical compositions of OPC and WBP.

Material	SiO_2	Fe_2O_3	Al_2O_3	CaO	MgO	Na_2O	K_2O	TiO_2	MnO	P_2O_5	Ba	S	LOI
Cement	15.45	4.55	2.81	62.45	–	0.48	1.01	0.47	0.12	1.29	0.05	2.75	7.47
WBP	64.36	12.86	8.71	2.00	–	1.82	3.05	2.13	0.68	1.18	1.18	–	0.97

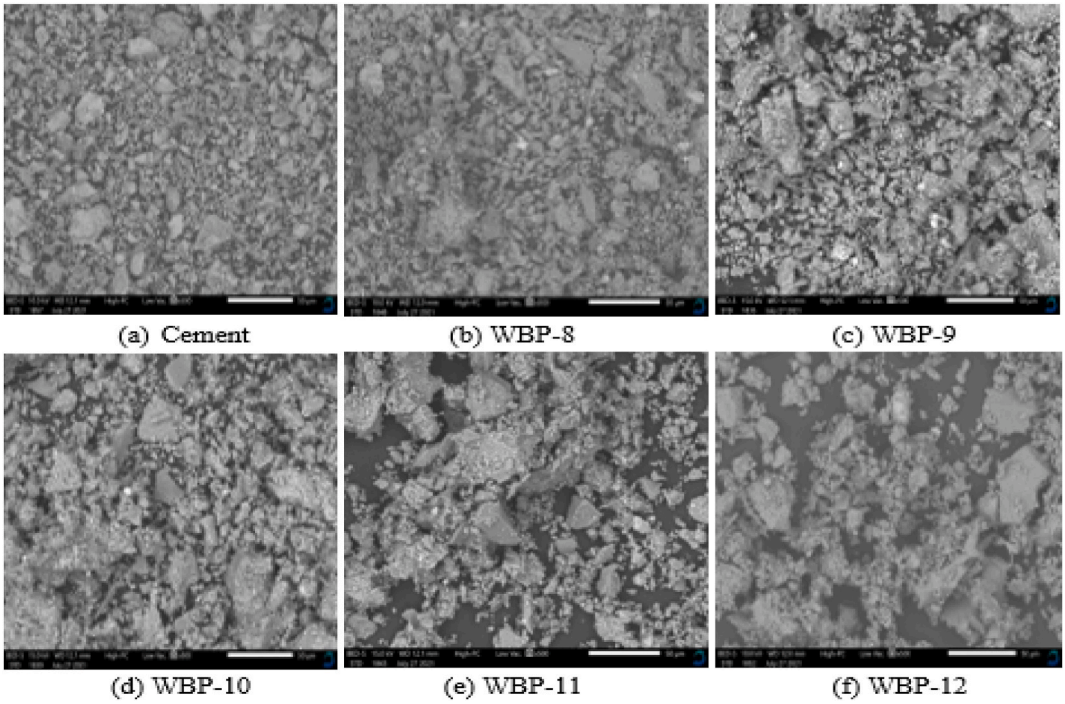

Fig. 2. Generated SEM micrographs of OPC and WBP specimens. Note that X in WBP-X specimens denotes the mass of clay bricks used during grinding to obtain WBP. Adapted from Ref. [75].

3.3. Shape parameters

3.3.1. Circularity

Fig. 3(a–f) reports the frequency distributions of the circularity characteristics of the specimens. Data in Table 4 indicate the means, standard deviations and confidence intervals of the circularity values of the specimens. Unlike Fig. 3(a–f), Fig. 4 shows the average circularity values of the specimens. Estimation of circularity of particles is vital in the evaluation of grain shape and this could provide significant insight on roundness of particles [15]. Generally, all the specimens illustrate the mean circularity values of higher than 0.59 suggesting that the majority of the particles of the specimens are approximately circular.

From Fig. 3(a–f), it is clear that most particles are characterised by circularity values ranging from 0.7 to 0.8 with the exception of WBP-11. For all the specimens, the lowest counts of circularity values are noticed with the range of 0–0.1. Quick visual impression of the frequency distributions illustrates that few particles are characterised by lower circularity values. It is important to mention that recognising the shape of the distribution is a vital technique in the evaluations of histograms of numerical values [76]. Using the constructed Gaussian distributions, it is explicit that all the frequency distributions illustrate that the average circularity values fall near to 0.6 for all the specimens. This observation is confirmed with values in Table 4. The fact that the histograms are skewed to the left seems to justify the validity of observing mean values of circularity of higher than 0.5. While not explicitly in agreement with the constructed normal distributions, the frequency distributions are seen not to be very far from the normal distributions. Although the Gaussian distributions used in this study are not very efficient in fitting the generated histograms, other distributions are proposed. It should also be noted that comprehensive statistical and probabilistic results in relation to Gaussian distributions have been deliberately avoided. Only simple statistical discussions have been thrown in for the sake of brevity.

The closeness of the circularity values to the mean can be obtained from the standard deviation and confidence interval values in Table 4 and the error bars in Fig. 4. The standard deviations are noticed to be high for the circularity values. The source of the high standard deviations, explaining the behaviour of high standard deviation, has been observed in the frequency counts in Fig. 3(a–f) where the frequency counts span from 0 to 1. From these findings, it can be noticed that the frequency counts' range of 30–350 is visible for circularity values ranging from 0.1 to 1. This is the reason why the solutions of standard deviations of circularity were able to attain increased values with the range of standard deviation values being 0.21–0.23. It should also be noted that the confidence interval values for the specimens are also high. Therefore, the high values of standard deviation and confidence interval both share the same vision that increased error bars could be produced for the circularity values.

Next, the performances of grinding conditions using changing masses of clay bricks introduced in ball mill are investigated in terms of their influence on circularity. Although grinding WBP using different masses of clay bricks occasioned significant changes in particle sizes, it is difficult to conclude from Figs. 3 (a–f) and 4 hat such milling conditions caused significant influence on circularity. It is suspected that even such changes in milling conditions may not bring benefits to the significant changes of particle shapes. These observations of insignificant effects of masses of clay bricks in ball mill run contrary to the observations of fineness levels of the

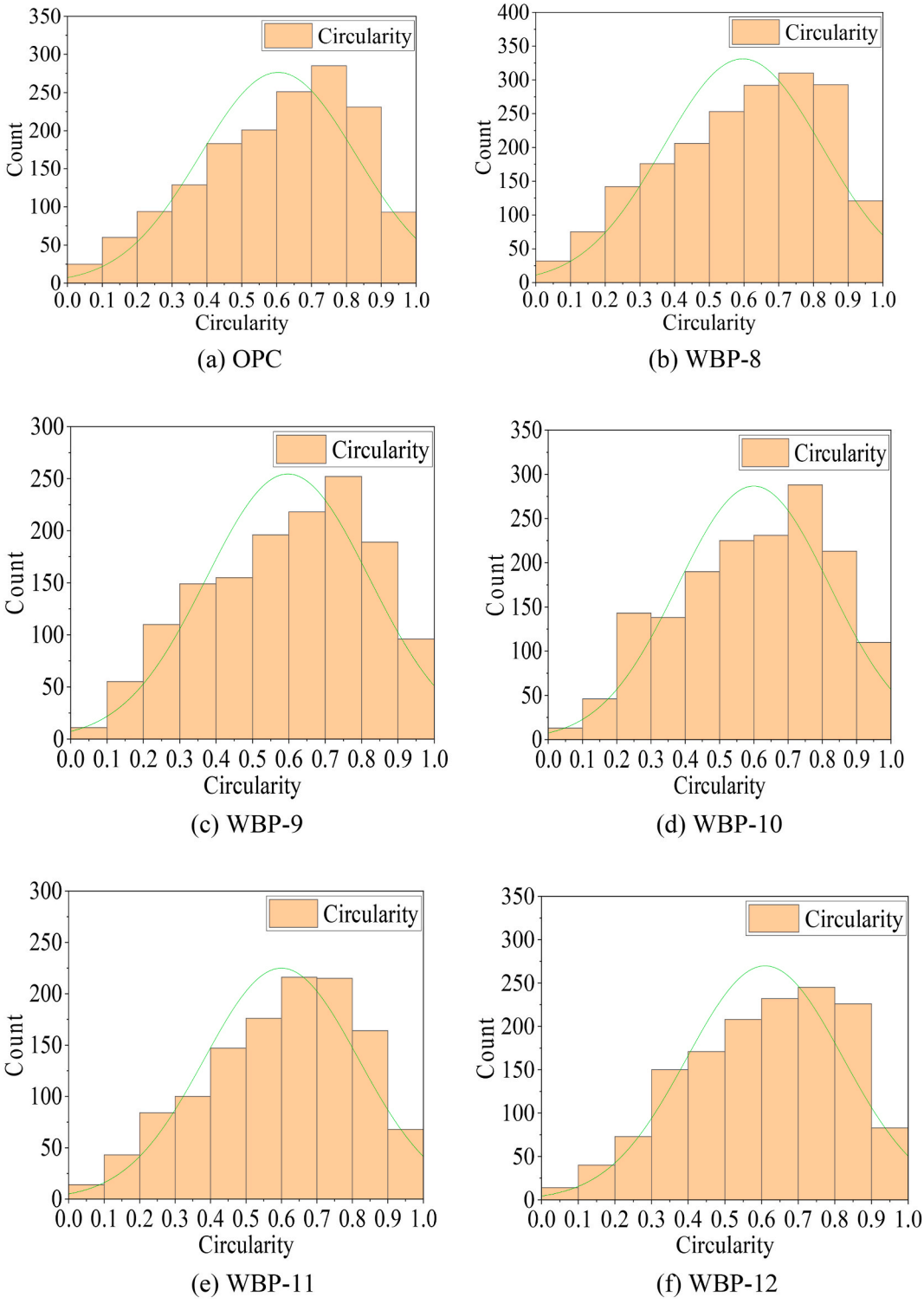

Fig. 3. Frequency distributions of circularity values of the specimens. Note that the green curve reports the Gaussian distribution for circularity counts. (For interpretation of the references to colour in this figure legend, the reader is referred to the Web version of this article.)

generated WBP. However, close examination of the values in Table 4 shows that the differences in the mean circularity values are not substantial. The small range of average circularity values of 0.0121787 suggests that the average circularity values of the specimens are barely different. Other researchers [77], reported that milling will likely influence the shapes of the particles. In spite of this reported

Table 4
Generated statistical parameters of circularity values of the specimens.

Parameter	Specimen					
	OPC	WBP-8	WBP-9	WBP-10	WBP-11	WBP-12
Mean	0.6044504	0.5975659	0.5973857	0.5996719	0.6000065	0.6095645
Standard deviation	0.2240501	0.2287273	0.2243069	0.2221938	0.2176232	0.2132140
Confidence interval	0.0111554	0.0102966	0.0116316	0.0109058	0.0121888	0.0110140

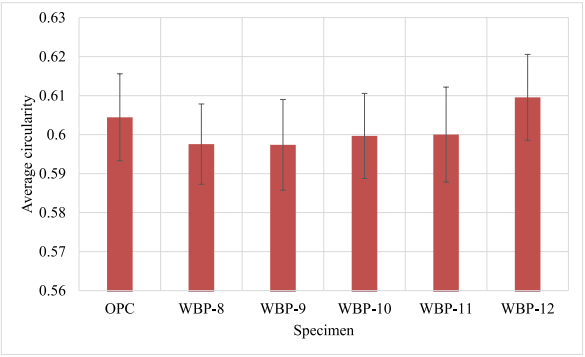

Fig. 4. Average circularity values of the specimens.

influence of grinding on particle shapes, the results of circularity of the specimens indicated in Fig. 4 do not differ much and no significant trends have been established. There is a high possibility that grinding in this study was not translatable to significant differences in particle shapes. The findings in this research may also explain why direct interpretation of particle shapes of specimens from changing milling conditions has not been straightforward in literature [78,79].

From Fig. 4, the specimen exhibiting the highest mean circularity value is WBP-12 while the specimen illustrating the lowest mean circularity value is WBP-9. The values of mean circularity in Fig. 4 seem to fail to give any indication of significant influence of grinding conditions on shapes of the particles. Such outcomes are also confirmed in Table 4. The question is if introductions of increasing masses of clay bricks in ball mill affected the circularity values of the WBP specimens. It is reasonable to presume that such insignificant variations illustrate that the findings of shape parameters are minimally sensitive to the masses of clay bricks introduced in ball mill. In fact, in Fig. 4, the average circularity values first decrease from WBP-8 to WBP-9, then slightly increase until WBP-11 and finally steeply increase from WBP-11 to WBP-12. Another case study is considered in Table 4 which reports the average circularity value of OPC. This average circularity value of OPC is less than that of WBP-12 but higher than the remaining specimens investigated. In truth, it is difficult to compare the circularity values between OPC and WBP considering the different generation approaches used for the two materials. However, as shown in Fig. 4 and Table 4, it is clear that OPC particles can recover average circularity values higher than 0.59 as is the case with the WBP specimens.

When developing shape parameters of pozzolanic materials, it is also important to mention their significance in cement-based composites. One crucial advantage of shape parameters is that they can influence the properties of cement-based composites [11]. Most notably, the particles of pozzolans that are not circular have been noticed to influence the water demand of cementitious composites [4]. The significant changes of water demand of cement-based composites incorporating WBP generated in this study can be inferred from the fact that the particles of WBP are not circular.

3.3.2. Solidity

Fig. 5(a–f) shows the frequency counts of the solidity values for the WBP specimens and cement. The analysis of the generated frequency counts is conducted with the accompanying details in Fig. 6 and Table 5. The adopted strategy of embedding the frequency count approach within the frameworks of data in Fig. 6 and Table 5 has been utilised in several applications because of its effectiveness in data evaluation. The findings on solidity demonstrate that they are similar to those for circularity previously presented, both not being able to generate significant trends among the specimens.

With respect to the normal distributions in Fig. 5(a–f), they are approximated representations of the frequency distributions. In the illustrated distributions, the mean solidity values are nearly 0.7. Such information has been inherited from Table 5 where the mean solidity values of the specimens are also noticed to be approximately 0.7. All these approaches are the basis of the fact that grinding clay bricks generated the particles of high solidity values. The high values of solidity for the specimens are therefore the consequences of grinding clay bricks using different masses but do not necessarily mean that such grinding conditions ensured the significant influence on solidity. In passing, it is noted that the highest counts of solidity values are observed with the range of 0.65–0.7 for all the specimens, thereby confirming the reason why the mean solidity values are approximately 0.7. It should be remembered that the clay bricks with changing masses introduced in ball mill spent the constant residence time of 1 h in ball mill. This condition reinforces the

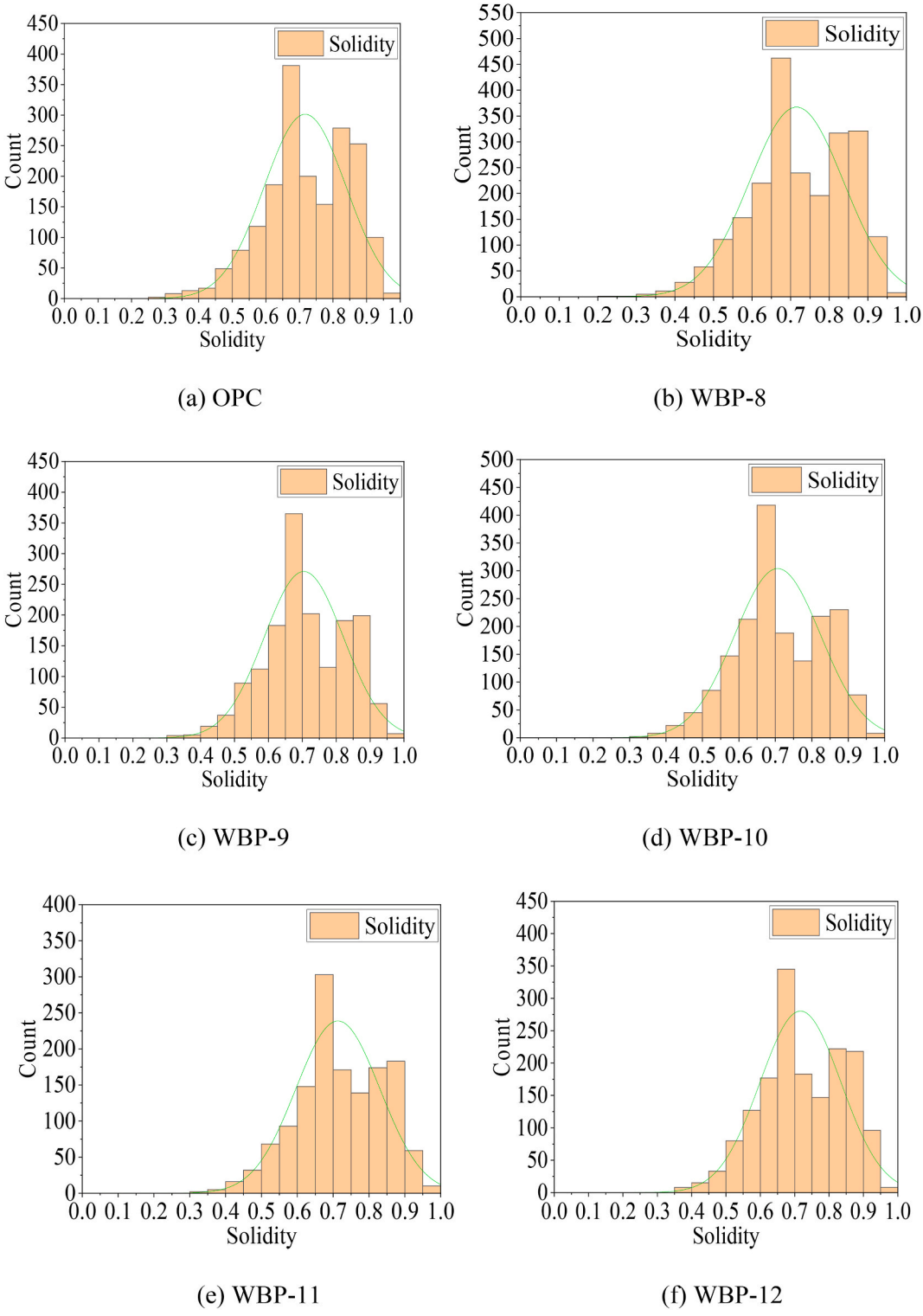

Fig. 5. Frequency distributions of solidity values of the specimens. Note that the green curve reports the Gaussian distribution for solidity counts. (For interpretation of the references to colour in this figure legend, the reader is referred to the Web version of this article.)

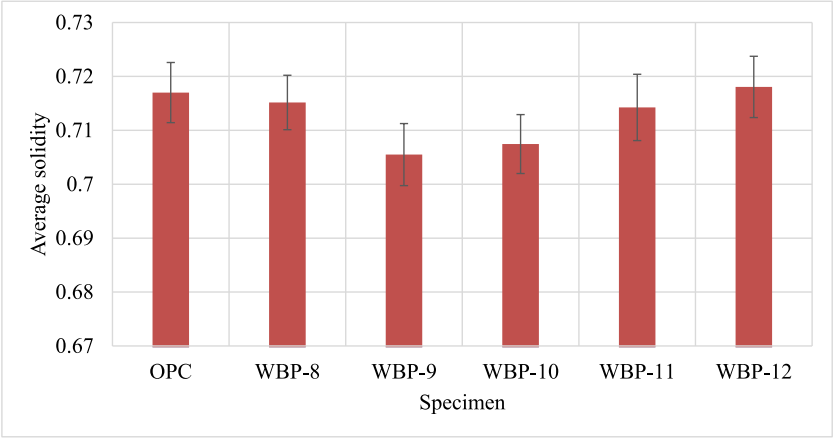

Fig. 6. Average solidity values of the specimens.

Table 5
Generated statistical parameters of solidity values of the specimens.

Parameter	Specimen					
	OPC	WBP-8	WBP-9	WBP-10	WBP-11	WBP-12
Mean	0.7170060	0.7151664	0.7054987	0.7074541	0.7142480	0.7180530
Standard deviation	0.1223028	0.1221161	0.1168080	0.1181949	0.1174433	0.1180895
Confidence interval	0.0055798	0.0050508	0.0057567	0.0054654	0.0061507	0.0056866

belief that there was no interference of milling time on the properties of the generated WBP. It is also important to mention that the standard deviations of the solidity values are less than those for circularity values previously explained. The same holds true for the error bars of average solidity values in Fig. 6 and those for circularity in Fig. 4. This seems to be due to the fundamental role of reduced range of solidity values (i.e. 0.3–1) compared with the range of 0.1–1 for circularity. This appears to be relevant and it seemed to have allowed the standard deviations to benefit from such reduced range.

It is important to highlight that shape descriptors if chosen wisely, present quantitative, reproducible and significant details of the particle morphology [39]. Circularity and solidity characteristics of particles are known to be the most significant morphological attributes [41]. Before moving on to other details of solidity values of the specimens, it is important to compare findings of solidity with circularity values previously presented. It is clear that the values of average solidity in Fig. 6 are greater than those for circularity in Fig. 4. Despite these differences, the findings of solidity are considered to be coherent with circularity findings. Noteworthy is the fact that the computations use the areas of the specimens. The distinctions are noticed with the remaining parameters which are perimeter for circularity and convex area for solidity. As clearly shown in the findings, the increments in the particle perimeters and convex areas during the computations of circularity and solidity respectively, led to the reductions of values for both shape parameters. Such conditions are encapsulated in Table 1. The findings seem to suggest that the increments in convex areas of particles caused minor deviations from solidity value of 1, in contrast with increments in perimeter values which resulted in higher deviations from circularity value of 1. In addition, the use of similar specimens during the computations in this study can the basis of the conclusions drawn between circularity and solidity values. Such consideration of same specimens opens doors to validity of comparisons among the shape parameters.

Interestingly, Table 5 illustrates that the standard deviations are not very high. Using the standard deviation values, it is easily noticed that the data sets of solidity values for the specimens are closer to the associated mean values. These outcomes are due to the increasing counts of solidity values close to the mean values, as it can quantitatively be noticed in Fig. 6. Again, the fact that the range illustrating the highest frequency counts in Fig. 5(a–f) is 0.65–0.7 seems to validate the findings on standard deviations. However, the influence of grinding clay bricks using different masses does not predict very well the statistical values of solidity. As it can be observed in Table 5, no significant trends are noticed with the values of mean, standard deviation and confidence interval under consideration of changing masses introduced in ball mill. This casts some doubts on the significant influence of increasing the masses of clay bricks introduced in ball mill on solidity values of WBP. As previously noted with circularity, less obvious is if changing the sample masses of clay bricks plays a significant role on the particle shapes of the generated WBP. Although previous study [75], captured significant reductions of fineness levels and grinding outputs of WBP following increments in the masses of clay bricks introduced in ball mill, this strategy has not influenced the solidity values in this study. For the former findings, these have been attributed to reductions of grinding impacts associated with increased masses of clay bricks introduced in ball mill [75]. For the latter findings, literature on the influence of these grinding environments on shape parameters is very scarce.

Whether the presented solidity findings of WBP particles can predict the behaviour of cementitious composites was also

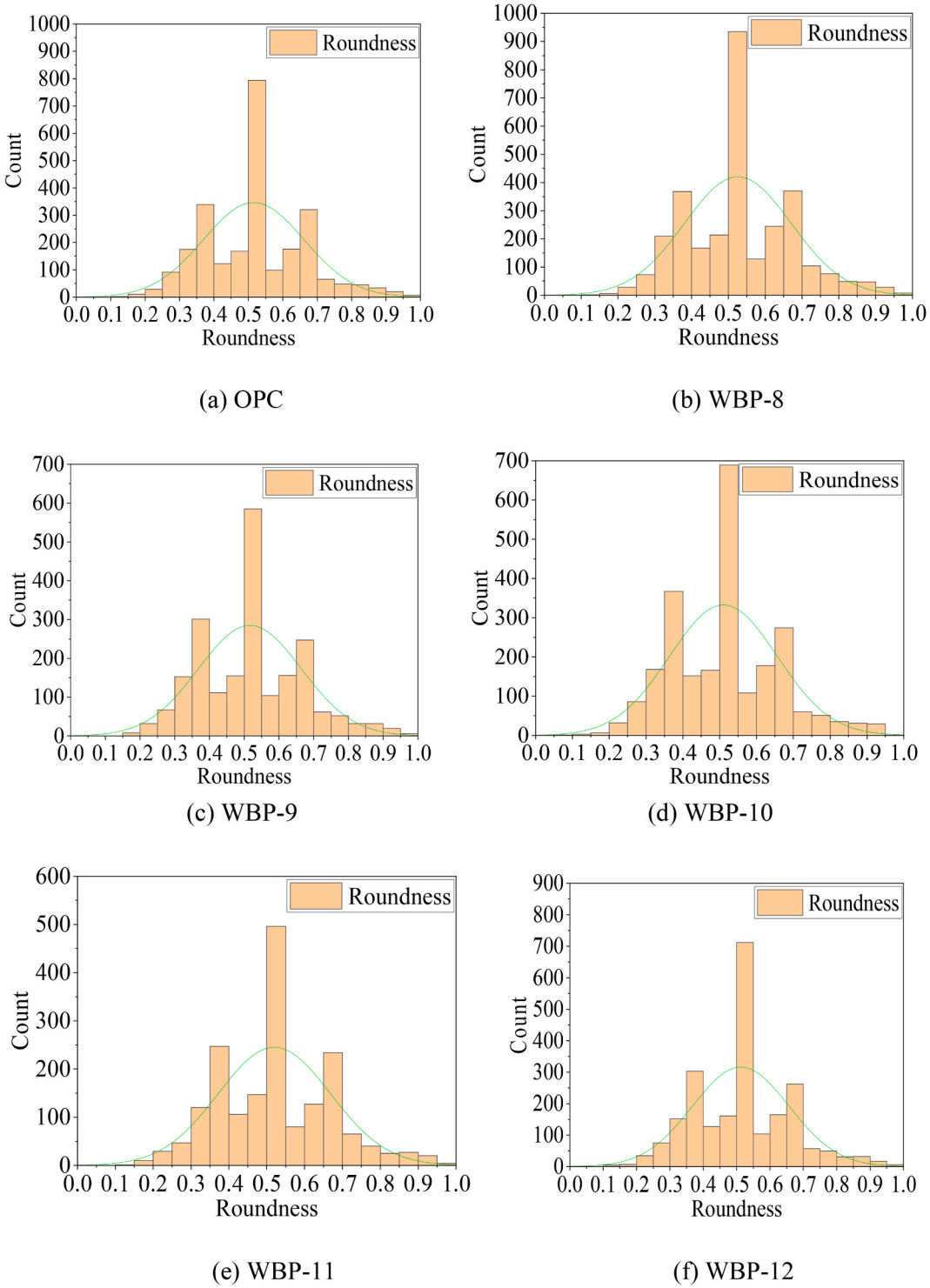

Fig. 7. Frequency distributions of roundness values of the specimens. Note that the green curve reports the Gaussian distribution for roundness counts. (For interpretation of the references to colour in this figure legend, the reader is referred to the Web version of this article.)

investigated in this study. The findings indicate that the solidity values deviate from 1, meaning that rough particle outlines were generated for the WBP particles. These findings and their explicit sensitivity to rough particle outlines, indicate that it would not be difficult for WBP to influence the workability properties of cement-based composites. The significant impact of particle shapes of pozzolans on properties of cement-based composites has been reported elsewhere [56].

3.3.3. Roundness

Fig. 7(a–f) shows the frequency counts of the roundness values for WBP and cement. In order to demonstrate the versatility of the frequency count approach, the Gaussian distribution is conceived for obtaining the distributions of the roundness values. The Gaussian distribution investigates the significance of the components of the histograms, both in relation to the accuracy of the distribution and computational outputs of the frequency counts. In Table 6 and Fig. 8, the generated data from the distribution and average roundness values are exhibited respectively. The considerations of insignificant trends traced for roundness values of the specimens from changing masses of WBP are also confirmed as were the cases with solidity and circularity values, although some distinctions arise because of computational differences for the shape parameters.

The results on roundness values of the investigated specimens in Fig. 7(a–f) assess the influence of grinding clay bricks using changing specimen masses. In all the reported cases in Fig. 7(a–f), the trends of histograms seem to obey the Gaussian distribution. From the numerical point of view, the range of mean roundness values of 0.510–0.525 provides evidence for the excellent agreement with the Gaussian distribution. As reference, the results are also compared with solidity and circularity values previously presented. The average roundness values are noticed to be the lowest among the three investigated shape parameters. Although roundness is reported to be similar to circularity [80], significant differences between average values of roundness and circularity are noticed. Between the average circularity and roundness values, never are the differences less than 0.07. Addressing the significant differences between roundness and circularity lies in the variable of perimeter for circularity and major axis for roundness. Significant differences between perimeter and major axis values of the particles might have probably led to the significant differences in circularity and roundness values. Again, such differences are encapsulated in Table 1.

It is shown in Table 6 that, with the reduced standard deviations of roundness values, the reduced standard error bars could be realistically obtainable in return. The range of standard deviations is noticed as 0.145–0.149 and it seems highly probable that this resulted in reduced error bars in Fig. 8. All the standard deviation values for roundness values are noticed to lie between the afore-discussed circularity and solidity values. However, the range of roundness values is still very high (i.e. 0 – 1) similar to that of circularity values. Although the high range of circularity values resulted to increased standard deviations, this was not the same with roundness values. Therefore, the strategy of using high range of roundness values should not be trusted in interpretation of roundness values. This strategy can still be relevant in other applications like those of circularity but it is not very accurate. The condition of roundness values would oblige to use confidence interval values. Since the confidence interval values of roundness are less than those for circularity values, the reduced standard deviation values for roundness are justified.

The analysis of influence of reduced particle sizes of WBP on roundness of the particles has been conducted and no significant trend has been established. It seems that the grinding conditions used in this study had negligibly little impact or no impact on the shape parameters of WBP. However, the grinding outputs and fineness levels of WBP have been noticed to benefit from grinding using reduced masses of clay bricks introduced in ball mill [75]. This has been attributed to the increased forces from the grinding media associated with reduced masses of clay bricks introduced in ball mill [75]. In another study [81], reduced particle sizes of magnetite by ball milling was noticed to decrease the relative width and roundness of the particles. In this cited study, it was indicated that particle shapes do not only depend on grinding technique but also the crystal lattice and material specifications of the specimens. To thoroughly investigate the reasons for insignificant influence of grinding conditions on roundness values in this study, the individual average values of roundness have been shown in Fig. 8 and Table 6. First of all, it can be noticed that there is a decreasing trend of roundness values for WBP-8, WBP-9 and WBP-10 and this runs contrary to the observation in the previous study [81]. After WBP-10, the trend tends to increase and finally decrease. This could be an indication that the trend of roundness of the WBP did not perform well using changing milling treatments, despite the significant reductions of grinding outputs and fineness levels as the masses of clay bricks introduced in ball mall increased. Secondly, it is extremely important to notice that contradicting information does exist on the effect of grinding on particle shapes in literature and this makes it challenging to understand the importance of the phenomenon. For instance, other researchers [82], noticed that particle shape was not very important during the maximum recoveries of fluorite ore samples irrespective of grinding conditions. On the other hand, roundness seemed to be important than size for the recovery of scheelite ore samples. The selectivity of the importance levels of the samples led to the recommendation of avoiding general conclusions on the subject. Based on the findings in this research, it seemed unlikely that the grinding conditions led to significant trends in roundness of WBP specimens. It is important to mention that this research could have benefited from other charaterisation methods of shape descriptors instead of 2-d shape parameters used in this study. As a final remark, the research community can therefore use such characterisation methods to broaden the understanding of shape parameters under changing milling conditions.

4. Conclusions

This research has presented quantitative image analysis approach that leverages data from scanning electron microscopy to generate the shape parameters of waste brick powder specimens subjected to changing milling treatments. This study has therefore identified the following important conclusions.

Table 6
Generated statistical parameters of roundness values of the specimens.

Parameter	Specimen					
	OPC	WBP-8	WBP-9	WBP-10	WBP-11	WBP-12
Mean	0.5153868	0.5256305	0.5163384	0.5101682	0.5201008	0.5125620
Standard deviation	0.1464841	0.1451669	0.1484079	0.1461254	0.1485122	0.1449381
Confidence interval	0.0056949	0.0051472	0.0063180	0.0058045	0.0068182	0.0059278

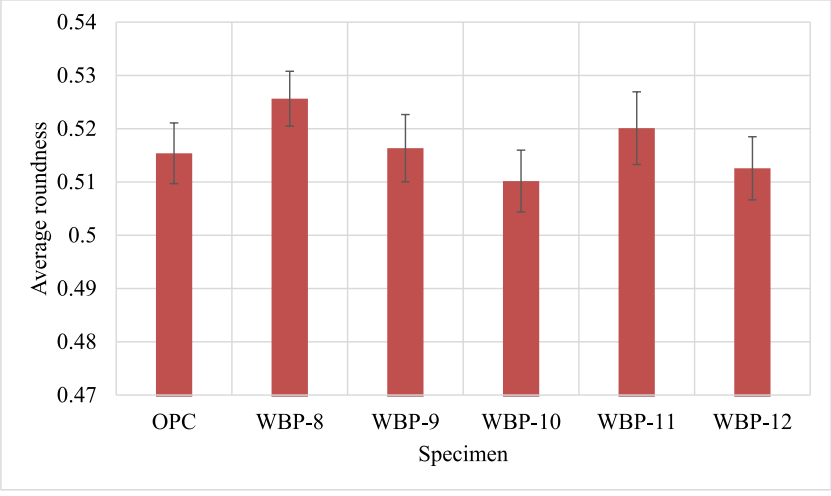

Fig. 8. Average roundness values of the specimens.

1. The findings in this study seem to indicate that quantitative image analysis strategy is robust and versatile in generating information of shape parameters of WBP. This strategy is capable of inheriting detailed information from scanning electron microscopy micrographs. These capabilities provide insights for predicting the influence of WBP on cement-based composites.
2. The results of average circularity, solidity and roundness values of greater than 0.5 indicate the likelihood of WBP in influencing the properties of cement-based composites.
3. The quantified values of circularity, solidity and roundness collaborate to support the discoveries of hidden shape characteristics of WBP specimens and can potentially tackle the overall behaviour of cement-based composites containing WBP.
4. It was shown that no significant trends in the investigated shape parameters could be developed under different milling conditions. In this regard, other approaches should be incorporated in future to better predict the impact of the varying milling conditions.
5. Some general conclusions generated in this study could be applied as the basis for further studies on particle shapes of WBP under changing conditions of milling.

CRediT authorship contribution statement

David Sinkhonde: Writing – review & editing, Writing – original draft, Visualization, Validation, Software, Resources, Project administration, Methodology, Investigation, Funding acquisition, Formal analysis, Data curation, Conceptualization.

Declaration of competing interest

The author declares that he has no known competing financial interests or personal relationships that could have appeared to influence the work reported in this paper.

Acknowledgements

This research was supported by the Pan African University Institute for Basic Sciences, Technology and Innovation (PAUSTI) during the Master of Science in Civil Engineering Training of the author.

References

[1] D. Sinkhonde, A. Rimbarngaye, B. Kone, T.C. Herring, Representativity of morphological measurements and 2-d shape descriptors on mineral admixtures, Results Eng 13 (2022) 100368.
[2] E. Berrezueta, J. Cuervas-Mons, Á. Rodríguez-Rey, B. Ordóñez-Casado, Representativity of 2D shape parameters for mineral particles in quantitative petrography, Minerals 9 (12) (2019).
[3] American Coal Ash Association, Fly ash facts for highway engineers, J. Chem. Inf. Model. 53 (9) (2013) 1689–1699.
[4] D.K. Panesar, Supplementary Cementing Materials, Elsevier LTD, 2019.
[5] M.C.G. Juenger, R. Siddique, Recent advances in understanding the role of supplementary cementitious materials in concrete, Cement Concr. Res. 78 (2015) 71–80.
[6] R. Siddique, J. Klaus, Influence of metakaolin on the properties of mortar and concrete: a review, Appl. Clay Sci. 43 (3–4) (2009) 392–400.
[7] C.F. Ferraris, K.H. Obla, R. Hill, The influence of mineral admixtures on the rheology of cement paste and concrete, Cement Concr. Res. 31 (2) (2001) 245–255.
[8] D. Jiao, C. Shi, Q. Yuan, X. An, Y. Liu, H. Li, Effect of constituents on rheological properties of fresh concrete-A review, Cem. Concr. Compos. 83 (2017) 146–159.
[9] M.I. Khan, R. Siddique, Utilization of silica fume in concrete: review of durability properties, Resour. Conserv. Recycl. 57 (2011) 30–35.
[10] M. Thomas, The effect of supplementary cementing materials on alkali-silica reaction: a review, Cement Concr. Res. 41 (12) (2011) 1224–1231.
[11] R. Walker, S. Pavía, Physical properties and reactivity of pozzolans, and their influence on the properties of lime-pozzolan pastes, Mater. Struct. Constr. 44 (6) (2011) 1139–1150.
[12] M. Mitterlehner, et al., Comparative evaluation of characterization methods for powders used in additive manufacturing, J. Mater. Eng. Perform. 30 (9) (2021) 7019–7034.
[13] U. Ulusoy, A review of particle shape effects on material properties for various engineering applications: from macro to nanoscale, Minerals 13 (1) (2023).
[14] P. Singh, P. Ramakrishnan, Review powder characterization by particle shape assessment, KONA Powder Part. J. 14 (14) (1996) 16–30.
[15] D.A. Tuan, V.T. Tung, L. Van Phuong, Analyzing 2D structure images of piezoelectric ceramics using ImageJ, Int. J. Mater. Chem. 4 (4) (2014) 88–91.
[16] E.J. Garboczi, N. Hrabe, Particle shape and size analysis for metal powders used for additive manufacturing: technique description and application to two gas-atomized and plasma-atomized Ti64 powders, Addit. Manuf. 31 (November 2019) (2020) 100965.
[17] A. Hejduk, S. Czajka, J. Lulek, Impact of co-processed excipient particles solidity and circularity on critical quality attributes of orodispersible minitablets, Powder Technol. 387 (2021) 494–508.
[18] R. Hela, D. Orsakova, The mechanical activation of fly ash, Procedia Eng. 65 (2013) 87–93.
[19] M. Li, et al., A bioinspired alginate-gum Arabic Hydrogel with micro-/Nanoscale structures for controlled drug release in chronic wound healing, ACS Appl. Mater. Interfaces 9 (27) (2017) 1–32.
[20] K. Ganesan, K. Rajagopal, K. Thangavel, Rice husk ash blended cement: assessment of optimal level of replacement for strength and permeability properties of concrete, Construct. Build. Mater. 22 (8) (2008) 1675–1683.
[21] M.M. Al-Ansari, N.D. Al-Dahmash, A.J.A. Ranjitsingh, Synthesis of silver nanoparticles using gum Arabic: evaluation of its inhibitory action on Streptococcus mutans causing dental caries and endocarditis, J. Infect. Public Health 14 (3) (2021) 324–330.
[22] N.L. Thomas, J.D. Birchall, The retarding action of sugars on cement hydration, Cem. Concr. Compos. 13 (1983) 830–842.
[23] K. Gunasekaran, R. Annadurai, P.S. Kumar, Study on reinforced lightweight coconut shell concrete beam behavior under flexure, Mater. Des. 46 (2013) 157–167.
[24] O.M. Olofinnade, A.N. Ede, J.M. Ndambuki, G.O. Bamigboye, Structural properties of concrete containing ground waste clay brick powder as partial substitute for cement, Mater. Sci. Forum 866 (2016) 63–67.
[25] M.J. Al-kheetan, M.M. Rahman, S.H. Ghaffar, M. Al-tarawneh, Y.S. Jweihan, Comprehensive investigation of the long-term performance of internally integrated concrete pavement with sodium acetate, Results Eng 6 (2020).
[26] R.C. Joshi, Pozzolanic Reactions in Synthetic Fly Ashes,, PhD Thesis, Iowa State University, Iowa, USA, 1970.
[27] Z.X. Zang, C.G. Yan, Z.Y. Dong, J. Huang, Y.F. Zang, Granger causality analysis implementation on MATLAB: a graphic user interface toolkit for fMRI data processing, J. Neurosci. Methods 203 (2) (2012) 418–426.
[28] E. Berrezueta, L. González-Menéndez, B. Ordóñez-Casado, P. Olaya, Pore network quantification of sandstones under experimental CO2 injection using image analysis, Comput. Geosci. 77 (2015) 97–110.
[29] K. Liu, M. Ostadhassan, Multi-scale fractal analysis of pores in shale rocks, J. Appl. Geophys. 140 (2017) 1–10.
[30] C. Igathinathane, L.O. Pordesimo, E.P. Columbus, W.D. Batchelor, S.R. Methuku, Shape identification and particles size distribution from basic shape parameters using ImageJ, Comput. Electron. Agric. 3 (2008) 168–182.
[31] M.H.N. Yio, Characterising the Microstructure of Cement-Based Materials Using Laser Scanning Confocal Microscopy,, PhD Thesis, Imperial College London, London, 2017.
[32] T.J. Collins, ImageJ for microscopy, Biotechniques 43 (1) (2007) 25–30.
[33] J. Bandyopadhyay, S.S. Ray, The quantitative analysis of nano-clay dispersion in polymer nanocomposites by small angle X-ray scattering combined with electron microscopy, Polymer (Guildf). 51 (6) (2010) 1437–1449.
[34] R. Lind, Open Source Software for Image Processing and Analysis: Picture This with ImageJ, Woodhead Publishing Limited, Cambridge, England, 2012.
[35] E.C. Crawford, J.K. Mortensen, An ImageJ1 plugin for the rapid morphological characterization of separated particles and an initial application to placer gold analysis, Comput. Geosci. 35 (2009) 347–359.
[36] J. Zhu, R. Balieu, X. Lu, N. Kringos, Microstructure evaluation of polymer-modified bitumen by image analysis using two-dimensional fast Fourier transform, Mater. Des. 137 (2018) 164–175.
[37] M. Vippola, M. Valkonen, E. Sarlin, M. Honkanen, H. Huttunen, Insight to nanoparticle size analysis — novel and convenient image analysis method versus conventional techniques, Nanoscale Res. Lett. (6–11) (2016).
[38] S. Sinha Ray, Structure and Morphology Characterization Techniques. Clay-Containing Polymer Nanocomposites, 2013.
[39] E.J. Liu, K. V Cashman, A.C. Rust, Optimising shape analysis to quantify volcanic ash morphology, GeoResJ 8 (2015) 14–30.
[40] J.R. Grace, A. Ebneyamini, Connecting particle sphericity and circularity, Particuology 54 (2021) 1–4.
[41] A. Hejduk, S. Czajka, J. Lulek, Impact of co-processed excipient particles solidity and circularity on critical quality attributes of orodispersible minitablets, Powder Technol. 387 (2021) 494–508.
[42] B.V.V. Reddy, M. Mani, P. Walker, Earthen Dwellings and Structures, Springer, Singapore, 2019.
[43] Z. Ge, Y. Wang, R. Sun, X. Wu, Y. Guan, Influence of ground waste clay brick on properties of fresh and hardened concrete, Construct. Build. Mater. 98 (2015) 128–136.
[44] D. Oni, J. Mwero, C. Kabubo, Experimental investigation of the physical and mechanical properties of Cassava Starch modified concrete, Open Construct. Build Technol. J. 13 (1) (2020) 331–343.
[45] A. Alsalman, L.N. Assi, R.S. Kareem, K. Carter, P. Ziehl, Energy and CO2 emission assessments of alkali-activated concrete and Ordinary Portland Cement concrete: a comparative analysis of different grades of concrete, Clean. Environ. Syst. 3 (2021) 100047.
[46] F. Bektas, K. Wang, Performance of ground clay brick in ASR-affected concrete: effects on expansion , mechanical properties and ASR gel chemistry, Cem. Concr. Compos. (1–6) (2011).
[47] C. V Israel, Rapid Characterization of Raw Materials for the Production of Concrete Admixtures (Part 1). Hefer Valley, Israel, BFT International, 2021.
[48] M.J. McCarthy, T.D. Dyer, Pozzolanas and Pozzolanic Materials, fifth ed., Elsevier Ltd., 2019.
[49] V. Sata, C. Jaturapitakkul, K. Kiattikomol, Influence of pozzolan from various by-product materials on mechanical properties of high-strength concrete, Construct. Build. Mater. 21 (7) (2007) 1589–1598.
[50] C. Shi, Y. Wu, C. Riefler, H. Wang, Characteristics and pozzolanic reactivity of glass powders, Cement Concr. Res. 35 (5) (2005) 987–993.

[51] J. Shao, J. Gao, Y. Zhao, X. Chen, Study on the pozzolanic reaction of clay brick powder in blended cement pastes, Construct. Build. Mater. 213 (2019) 209–215.
[52] V.F. Rahhal, et al., Complex characterization and behavior of waste fired brick powder-portland cement system, Materials 12 (2019) 1–20.
[53] W. Xu, T.Y. Lo, S.A. Memon, Microstructure and reactivity of rich husk ash, Construct. Build. Mater. 29 (2012) 541–547.
[54] S.A. Zareei, F. Ameri, F. Dorostkar, M. Ahmadi, Rice husk ash as a partial replacement of cement in high strength concrete containing micro silica: evaluating durability and mechanical properties, Case Stud. Constr. Mater. 7 (2017) 73–81.
[55] R. Fernandez, F. Martirena, K.L. Scrivener, The origin of the pozzolanic activity of calcined clay minerals: a comparison between kaolinite, illite and montmorillonite, Cement Concr. Res. 41 (1) (2011) 113–122.
[56] Y. Zhao, J. Gao, C. Liu, X. Chen, Z. Xu, The particle-size effect of waste clay brick powder on its pozzolanic activity and properties of blended cement, J. Clean. Prod. 242 (2020) 118521.
[57] BS EN 197-1, Cement - Part 1: Composition, Specifications and Conformity Criteria for Common Cements, BSI, London, UK, 2000.
[58] M.S. Shackley, X-ray fluorescence spectrometry (XRF), Encycl. Archaeol. Sci. (1–5) (2018).
[59] ASTM C311/C311M, Standard Test Method for Sampling and Testing Fly Ash or Natural Pozzolans for Use in Portland-Cement Concrete, ASTM International, West Conshohocken, USA, 2013.
[60] S. Spiegelberg, A. Kozak, G. Braithwaite, Characterization of Physical, Chemical, and Mechanical Properties of UHMWPE, Third Edit. Elsevier Inc., 2016.
[61] N. Raval, R. Maheshwari, D. Kalyane, S.R. Youngren-Ortiz, M.B. Chougule, R.K. Tekade, Importance of Physicochemical Characterization of Nanoparticles in Pharmaceutical Product Development, Elsevier Inc., 2018.
[62] F.A. Almarzooqi, M.R.B. Bilal, M. Hassan, A comparative study of image analysis and porometry techniques for characterization of porous membranes, J. Mater. Sci. 51 (4) (2015) 2017–2032.
[63] Origin, Origin User Guide, 2019b - OriginLab, OriginLab Corporation, Northampton, MA, USA, 2019.
[64] R. Butter, P. Dellino, H. Raue, I. Sonder, B. Zimanowski, Stress-induced brittle fragmentation of magmatic melts: theory and experiments, J. Geophys. Res. 111 (2006) 1–10.
[65] S.C. Jordan, T. Dürig, R.A.F. Cas, B. Zimanowski, Processes controlling the shape of ash particles: results of statistical IPA, J. Volcanol. Geoth. Res. 288 (2014) 19–27.
[66] M.L. Hentschel, N.W. Page, Selection of descriptors for particle shape characterization, Part. Part. Syst. Char. 20 (2003) 25–38.
[67] E.J. Liu, K. V Cashman, A.C. Rust, S.R. Gislason, The role of bubbles in generating fine ash during hydromagmatic eruptions, Goelogy (2015) 1–6.
[68] ASTM C618, Standard Specification for Coal Fly Ash and Raw or Calcined Natural Pozzolan for Use in Concrete, ASTM International, West Conshohocken, USA, 2003.
[69] H. Kabir, R.D. Hooton, N.J. Popo, Evaluation of cement soundness using the ASTM C151 autoclave expansion test, Cement Concr. Res. 136 (5) (2020).
[70] F. Bektas, K. Wang, H. Ceylan, Use of ground clay brick as a pozzolanic material in concrete, J. ASTM Int. (JAI) 5 (10) (2008) 1–10.
[71] D. Sinkhonde, R.O. Onchiri, W.O. Oyawa, J.N. Mwero, Effect of waste clay brick powder on physical and mechanical properties of cement paste, Open Civ. Eng. J. 15 (2021) 370–380.
[72] Y. Zhao, J. Gao, G. Liu, X. Chen, Z. Xu, The particle size effect of waste clay brick powder on its pozzolanic activity and properties of blended cement, J. Clean. Prod. 242 (1) (2019).
[73] J.T. Orasugh, S.K. Ghosh, D. Chattopadhyay, Nanofiber-reinforced Biocomposites, 2020.
[74] P. Lin, S. Lin, P.C. Wang, R. Sridhar, Techniques for physicochemical characterization of nanomaterials, Biotechnol. Adv. 32 (4) (2013) 711–726.
[75] D. Sinkhonde, D. Mashava, Analysis of milling treatments of waste clay bricks effect on density and compressive strength of cement paste, Results Mater 16 (November) (2022) 100346.
[76] D.L. Mohr, W.J. Wilson, R.J. Freund, Data and statistics, in: Statistical Methods, Academic Press, Massachusetts, USA, 2022, pp. 1–64.
[77] G.H. Bagheri, C. Bonadonna, I. Manzella, P. Vonlanthen, On the characterization of size and shape of irregular particles, Powder Technol. 270 (2015) 141–153. Part A.
[78] A. Abazarpoor, M. Halali, Investigation on the particle size and shape of iron ore pellet feed using ball mill and HPGR grinding methods, Physicochem. Probl. Miner. Process. 53 (2) (2017) 908–919.
[79] P. Pourghahramani, E. Forssberg, Review of applied particle shape descriptors and produced particle shapes in grinding environments. Part II: the influence of comminution on the particle shape, Miner. Process. Extr. Metall. Rev. 26 (2) (2005) 167–186.
[80] M.J. Zdilla, S.A. Hatfield, K.A. McLean, L.M. Cyrus, J.M. Laslo, H.W. Lambert, Circularity, solidity, axes of a best fit ellipse, aspect ratio, and roundness of the foramen ovale: a morphometric analysis with neurosurgical considerations, J. Craniofac. Surg. 27 (1) (2016) 222–228.
[81] F. Dehghani, B. Rezaie, A. Sachan, T. Ghosh, Effects of grinding on particle shape: silica and magnetite, in: 2019 *SME Annu. Conf. Expo C. 121st Natl. West. Min. Conf.*, 2019, pp. 1–11. February.
[82] L. Pereira, et al., On the impact of grinding conditions in the flotation of semi-soluble salt-type mineral-containing ores: driven by surface or particle geometry effects? Int. J. Min. Sci. Technol. (1–18) (2023).